Analyst

Accepted Manuscript

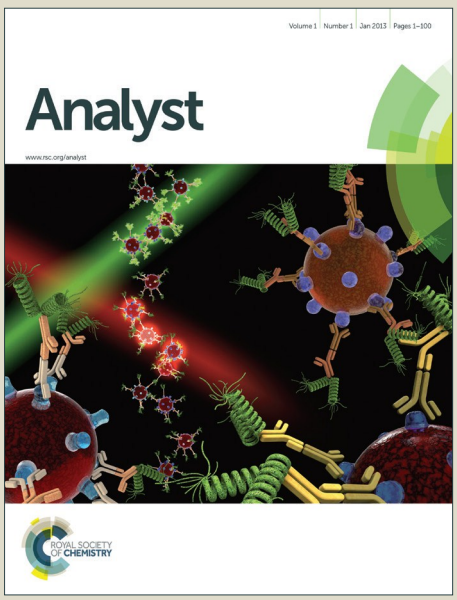

ROYAL SOCIETY OF CHEMISTRY

www.rsc.org/analyst

Journal Name

ARTICLE

Adsorption between TC-stabilized AuNPs and phosphate group: application for PTP1B activity assay

Received 00th January 20xx,
Accepted 00th January 20xx

DOI: 10.1039/x0xx00000x

www.rsc.org/

Jun Lv,[a] Xiaonan Wang,[a,b] Yuanyuan Zhang,[c] Defeng Li,[a] Juan Zhang*[a] and Lizhou Sun*[c]

Based on adsorption between tetracycline (TC) and phosphate groups, a general colorimetric method is explored in this work by using TC-stabilized gold nanoparticles (TC/AuNPs) and 4-aminophenyl phosphate-functionalized Fe_3O_4 magnetic nanoparticles (APP/MNPs). Take protein tyrosine phosphatase 1B (PTP1B) as an example, 4-aminophenyl phosphate (APP) can be hydrolyzed into 4-aminophenol (AP) by PTP1B, resulting in the disappearance of phosphate group at the outer layer of MNPs and the lost of corresponding adsorptive ability. Upon addition of TC/AuNPs solution, TC/AuNPs will remain in the supernatant solution after magnetic separation and a high absorbance value can be observed. So PTP1B activity is related to the concentrations of TC/AuNPs in the supernatant solution. In this work, the enzyme activity can be determined at levels as low as 0.0885 U/mL and over a linear detection range as wide as from 0.1 U/mL to 0.9 U/mL. Moreover, using the proposed method, the inhibition effect of betulinic acid (BA) and sodium orthovanadate (Na_3VO_4) on PTP1B activity can be tested with IC_{50} values of 30 μM and 4 μM, respectively. Therefore, a universal platform for accurate colorimetric analysis of kinases and phosphatases activities can be established through the adsorption between TC and phosphate groups.

1 Introduction

Protein phosphorylation and dephosphorylation can regulate the structures and functions of cellular proteins in a wide spectrum of cellular processes[1, 2]. Aberrant regulations in the cellular phosphoproteome network are implicated in most major human diseases[3, 4]. Consequently, kinases and phosphatases are two important drug targets in medicinal research today. It is of great importance for the recognition of phosphate groups in the detection of the enzymes activities. Currently, many techniques have been developed based on recognition of metal ions on phosphate groups. For instance, aluminium ions-immobilized iminodiacetate-agarose has been used as a chromatographic adsorbent to retain phosphoamino acids, phosphopeptides, phosphoproteins, and nucleotides that contained terminally bound phosphate[5]. Immobilized metal affinity chromatography is one of the most extensively used enrichment methods for phosphoproteomics analysis[6]. Otherwise, Zr^{4+} and Ti^{4+} have also been employed to substitute the common metals to enrich phosphopeptides[7, 8]. Similar to metal ion, tetracycline (TC), a wide-spectrum antibiotic, also shows the adsorptive capability on calcium phosphate apatites[9]. Meanwhile, its adsorption can be affected by phosphate on the soils[10]. However, the techniques have not been exploited based on the adsorption between TC and phosphate group.

It has been well confirmed that TC as a reducing agent can be used in synthesis of gold nanoparticles (AuNPs)[11], resulting in the stabilization of TC on the surface of AuNPs. Benefiting from the unique optical properties of AuNPs, many colorimetric methods have been widely established for testing different kinds of species like metal ions[12, 13], cells[14], proteins[15], and nucleic acids[16, 17]. However, the disperse state of AuNPs is easily susceptible to experimental conditions such as temperature, pH, salt concentration[18-20], and the charge of substance[21]. To overcome this drawback of AuNPs and avoid interference of substances, magnetic nanoparticals (MNPs) can be considered as an excellent choice due to its property of magnetic separation[22].

As an intracellular phosphatase, protein tyrosine phosphatase 1B (PTP1B) is responsible for negatively regulating insulin signaling by dephosphorylating the phosphotyrosine residues of the insulin receptor kinase activation segment[23]. Moreover, PTP1B can not only dephosphorylate the insulin receptor and insulin receptor substrate[24] but also dephosphorylate phosphotyrosyl residues of proteins and peptides[25]. Thereby, as a key negative regulator of the insulin signaling pathways, PTP1B plays important roles in down regulation of insulin and leptin signaling pathway. It is also an established therapeutic target for diabetes and obesity[26, 27]. Nowadays, several methods have been established to detect PTP1B activity. For example, *p*-nitrophenylphosphate (*p*NPP) has been traditionally chosen as the PTP1B substrate for UV-vis spectrometric method[28]. Meanwhile, the specific phosphotyrosyl peptides[29] and 3-nitrophosphotyrosine containing molecules[30] have also been

[a] *Laboratory of Biosensing Technology, School of Life Sciences, Shanghai University, Shanghai 200444, PR China. E-mail: juanzhang@shu.edu.cn; Fax: +86-21-66137541*
[b] *Shanghai Key Laboratory of Bio-Energy Crops, Shanghai University, Shanghai 200444, China.*
[c] *Department of Obstetrics and Gynecology, The First Affiliated Hospital of Nanjing Medical University, 210036 Nanjing, China. E-mail: lizhou_sun121@hotmail.com; Fax: +86-25-86663616*

explored as PTPs substrates for UV-vis spectroscopic measurement. Furthermore, fluorescence turn-on assays have been established for the detection of PTP1B activity[31, 32]. In this work, taking PTP1B as an example, we develop a versatile strategy to detect the enzymes involving in protein phosphorylation and dephosphorylation.

In our strategy, the adsorption between TC/AuNPs and phosphate group on the surface of magnetic nanoparticles (MNPs) is first exploited for the detection of PTP1B activity and the screening of its inhibitors. On the one hand, TC/AuNPs are prepared by one-step synthesis-modification strategy, using TC as the reduce reagent. Therefore, the as-prepared AuNPs are directly functionalized with TC in the particle synthesis, thus no more additional surface modification for introducing binding sites is needed in this strategy. The one-step preparation of functionalized AuNPs through synthesis-modification integration strategy is simpler in comparison with the conventional two-step fabrication methodology. On the other hand, magnetic separation eliminates the interfering substances so as to ensure the stability of TC/AuNPs and the accuracy of the assay.

2 Experimental

2.1 Materials and reagents

PTP1B (P6244), human recombinant, expressed in *E. coli* (30 U mg^{-1}), iron (Ⅲ) chloride, sodium tetraborate, N-(3-dimethylaminopropyl)-N'-ethylcarbodiimide hydrochloride (EDC), N-hydroxysuccinimide (NHS), chloroauric acid ($HAuCl_4 \cdot 3H_2O$), trisodium citrate, betulinic acid (BA), and sodium orthovanadate (Na_3VO_4) were purchased from Sigma (Shanghai, China). 4-aminophenylphosphate monosodium salt was purchased from Shanghai, LKT, Laboratories, Inc (Shanghai, China). Tetracyline hydrochloride and hexadecyltrimethylammonium chloride (CTAC) was purchased from Aladdin (Shanghai, China). All buffers and aqueous solutions were prepared with ultrapure water purified with a Millipore Milli-Q water purification system (Barnstead, USA) to a specific resistance of 18 MΩ·cm.

2.2 Preparation of TC/AuNPs

TC-stabilized AuNPs (TC/AuNPs) were synthesized according to the previous study[11]. Briefly, 1.2 mM $HAuCl_4$ solution with 2 mM CTAC as stabilizer in 10 mM sodium tetraborate buffer (pH 9.2) was mixed with TC solutions at a concentration of 0.087 mM. Solutions were incubated in the water bath at 70 °C for 10 min to obtain the final product, TC/AuNPs. After centrifugation, TC/AuNPs were dispersed in Tris-HCl buffer (50 mM, pH 5.6) and stored in a refrigerator at 4 °C.

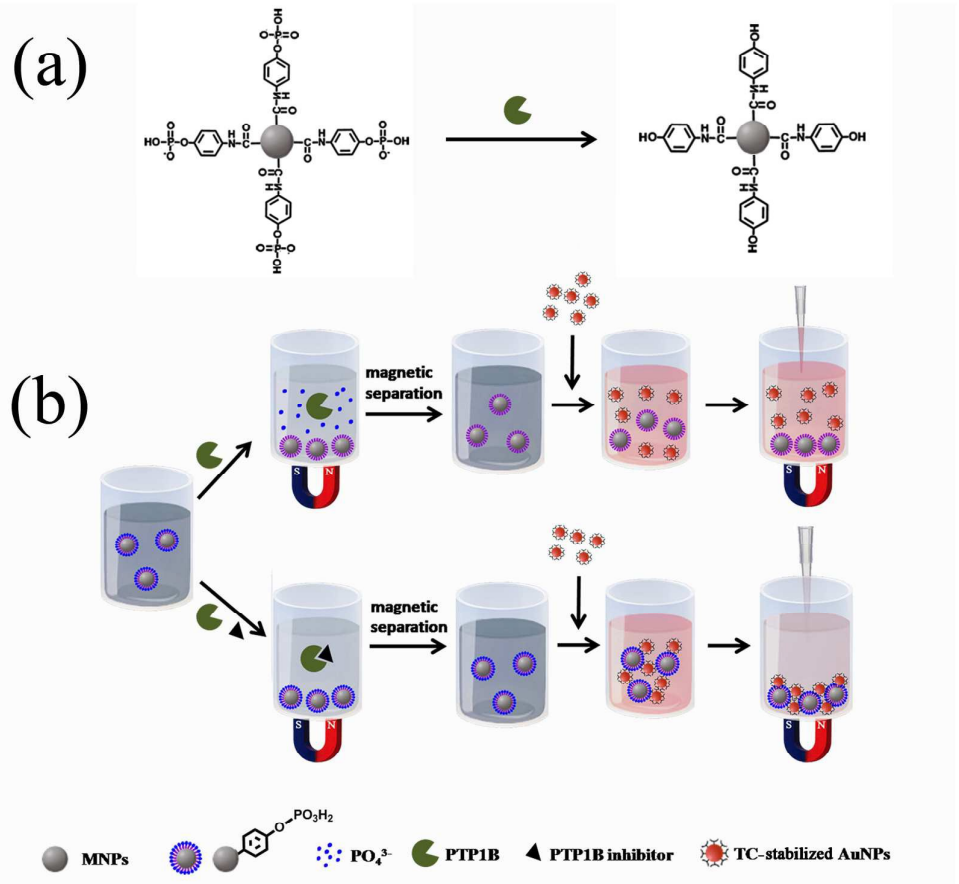

Scheme 1 Schematic illustration of the mechanisms for (a) PTP1B catalyzed reaction and (b) colorimetric determination of PTP1B activity and the inhibitors.

2.3 Synthesis of APP/MNPs

MNPs were synthesized by using a co-precipitation method[33]. Firstly, a 10 mL iron solution containing 0.5 M $FeSO_4$, 1 M $FeCl_3$, and 0.4 M HCl was prepared. Then, a 0.5 M NaOH solution (100 mL) was purged with nitrogen to remove oxygen and then heated to 80 °C. Subsequently, under rapid stirring, the iron solution was added drop by drop into NaOH solution. 80 min later, sodium citrate (1.94 M) was added and heated to 90 °C. The reaction mixture was further stirred for 60 min. After that, the precipitate was washed with water three times and isolated by magnetic decantation. The residue was finally made up to 50 mL with doubly distilled water, to give MNPs.

It has been well known that the three carboxylate groups of sodium citrate have strong coordination affinity to iron ions, which favours the attachment of citrate groups on the surface of the MNPs and the groups provide accessible surface for the conjugation of amino-terminated molecules[34]. A routine method[35] using EDC as a linker was employed to immobilize APP onto the surface of MNPs. Briefly, 0.22 M EDC and 0.22 M NHS were added into 1 mL MNPs and ultrasonicated for 30 min. After magnetic separation, 200 μL 0.4 mM APP aqueous solutions were added into MNPs with continuous stirring for 120 min. The resulting mixture was separated by using magnet and washed 3 times with deionized water, to give APP functionalized MNPs (APP/MNPs).

2.4 PTP1B activity assay

The PTP1B activity assay was performed using the following procedure. The PTP1B was firstly dissolved in 100 μL HEPES buffer solution (50 mM, pH 7.2) and then diluted at different concentrations with Tris-HCl buffer solution (50 mM, pH 7.2). After that, 10 μL enzyme solutions with different concentrations ranging from 0.1 to 1.7 U/mL were added into 40 μL of APP/MNPs solution and the resulting mixtures were allowed to stand at 30 °C for 20 min. Then, the modified MNPs were washed 2 times with deionized water to remove PTP1B and liberated phosphate groups after magnetic separation. After that, 80 μL TC/AuNPs solution was added into the resultant MNPs at room temperature. 20 min later, the supernatant solutions separated magnetically from the reaction mixture were used for UV-vis spectroscopic measurements and the absorbance values were recorded with a UV-vis spectrometer (Shimadzu Co., Kyoto, Japan).

2.5 Evaluation for Inhibitor assay

For the inhibition assay, BA or Na_3VO_4 aqueous solutions (10 μL) with different concentrations were first premixed with PTP1B (10 μL, 0.7 U/mL) for 10 min at 30 °C. Then APP/MNPs (40 μL) was added and the mixed solution was incubated for 20 min at 30 °C. After repeated washing and magnetic separation, 80 μL TC/AuNPs solution was added at room temperature for 20 min. Finally, the absorbance of the supernatant solution obtained after magnetic separation was recorded by using UV-vis spectroscopy and the IC_{50} value was calculated. The inhibitory ratio (%) of BA or Na_3VO_4 on PTP1B activity was calculated as follows:

$$\text{Inhibitory ratio}\,(\%) = \frac{A_1 - A}{A_1 - A_0} \times 100$$

where A_1 is the maximum absorbance value in the presence of the enzyme only, A is the maximum absorbance value in the presence of both enzyme and inhibitor, and A_0 is the maximum absorbance value in the absence of both enzyme and inhibitor.

3 Results and discussions

The principle of the colorimetric method is shown in Scheme 1. Firstly, APP, PTP1B substrate, is linked to MNPs through the formation of covalent amide bonds, to obtain the functionalized MNPs (APP/MNPs). PTP1B can hydrolyze APP/MNPs into 4-aminophenol modified MNPs (AP/MNPs) with the departure of phosphate group from the surface of MNPs into the solution (Scheme 1(a)). TC carrying a positive charge can attract negatively charged phosphate group through electrostatic interaction. It has been well confirmed that when the equilibrium solution pH is below 6, the predominant species of TC were TC^{+00} and $TC^{+-0\ 10}$. So, in the presence of PTP1B, the absorbance values of the supernatant solution after magnetic separation will keep unchanged as a result of the specific hydrolysis of APP into AP which contains no phosphate group and has no adsorptive capability with TC/AuNPs (Scheme 1(b)). On the contrary, in the absence of PTP1B, the values will decrease due to the adsorption between TC/AuNPs and APP/MNPs. Since PTP1B activity is related to the content of phosphate group at the outer layer of MNPs, a simple method for monitoring PTP1B activity through the change in the absorbance values of the supernatant solution, or even through direct observation by the naked eye can be developed. Moreover, this method can also be used to evaluate PTP1B inhibitors (Scheme 1(b)).

3.1 Characterization of TC/AuNPs and APP/MNPs

Fig. S1(a) and S1(b) separately show the TEM images of TC/AuNPs and APP/MNPs with the mean diameters of 14.52 nm ± 3.28 nm

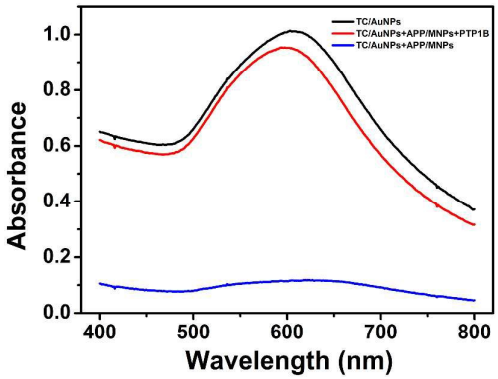

Fig. 1 UV-vis spectra of the mixtures prepared by separate addition of TC/AuNPs (80 μL) (black curve), TC/AuNPs (80 μL) + APP/MNPs (40 μL) + PTP1B (10 μL, 1.7 U/mL) (red curve) or TC/AuNPs (80 μL) + APP/MNPs (40 μL) (blue curve) to obtain the final volume of 130 μL with the addition of Tris-HCl buffer.

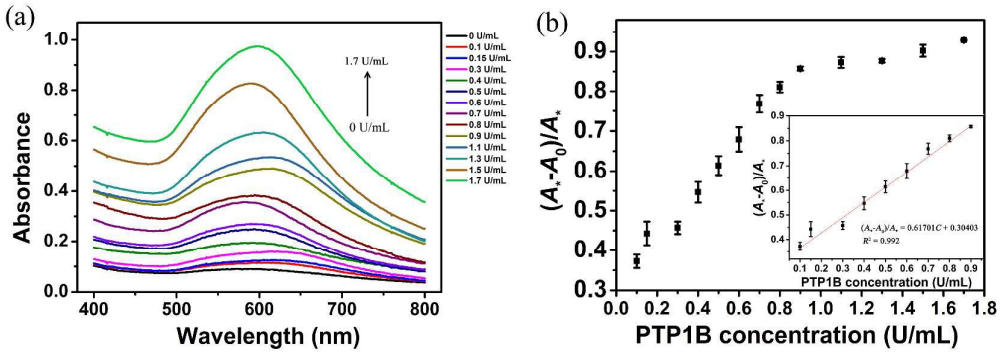

Fig. 2 (a) UV-vis spectra of supernatant solution of reaction mixture prepared by adding various concentrations of PTP1B (10 μL) into APP/MNPs (40 μL) followed by the addition of TC/AuNPs solution (80 μL). The PTP1B concentrations were 0.1, 0.15, 0.3, 0.4, 0.5, 0.6, 0.7, 0.8, 0.9, 1.1, 1.3, 1.5, and 1.7 U/mL. (b) Calibration curve corresponding to $(A_*\text{-}A_0)/A_*$ against the concentrations of PTP1B. Inset shows the linear relationship between $(A_*\text{-}A_0)/A_*$ values and the concentrations of PTP1B. A_* represents the maximum absorbance value at different concentrations of PTP1B, A_0 is the maximum absorbance value in the absence of PTP1B.

and 11.69 ± 2.94 nm, respectively. Compared to APP, APP/MNPs exhibit a new peak at 1414 cm^{-1} in the FT-IR spectrum (Fig. S1(c)), which belongs to the C-N stretching vibration. It well demonstrates that APP is successfully linked to MNPs through the formation of amide bonds. Meanwhile, in the FT-IR spectrum of TC/AuNPs, C=O stretching absorption peak exhibits a red shift from 1615 cm^{-1} to 1643 cm^{-1} in the comparison with that of TC, suggesting the occurrence of TC on the surface of AuNPs (Fig. S1(d)). Furthermore, TC shows two obvious absorption peaks at 275 nm and 357 nm in the UV-vis absorption spectrum (Fig. S1(e)). Meanwhile, the peak at 275 nm and the other, a characteristic absorption peak of AuNPs, appear simultaneously in the UV-vis spectrum of TC/AuNPs. These well indicate the formation of TC/AuNPs.

3.2 Investigation of adsorption between TC/AuNPs and APP/MNPs

As exhibited in Fig. 1, TC/AuNPs exhibits a strong absorption peak (black curve). Upon adding APP/MNPs into TC/AuNPs, a dramatic decrease for the absorption peak can be observed (blue curve). It can be well explained for the strong adsorption ability between TC and phosphate group at the outer layer of MNPs. However, with the addition of hydrolyzed product into TC/AuNPs, the absorption peak changes slightly (red curve). PTP1B can catalyze the cleavage of phosphate ester bond, resulting in the departure of phosphate group from the surface of MNPs and the formation of hydrolyzed product, AP/MNPs. AP/MNPs containing no phosphate group cannot adsorb with TC/AuNPs, so the absorbance value of supernatant solution almost remains unchanged after magnetic separation. These results are in accordance with our prediction and well demonstrate that the adsorption between TC/AuNPs and APP/MNPs can be used for PTP1B activity assay and the inhibitor screening.

3.3 PTP1B activity assay

As illustrated in Fig. 2(a), with the increase of the PTP1B concentrations from 0.1 U/mL to 1.7 U/mL, the absorbance values of supernatant solution increase gradually. It suggests the hydrolysis of APP/MNPs into AP/MNPs under PTP1B catalysis. AP/MNPs containing no phosphate group cannot adsorb TC/AuNPs. So after magnetic separation, the concentrations of TC/AuNPs in the supernatant solution increase and high absorbance values can be observed.

The $(A_*\text{-}A_0)/A_*$ values have been used for the quantitative detection of the PTP1B activity (Fig. 2 (b)). The values show a linear response toward PTP1B concentrations ranging from 0.1 U/mL to 0.9 U/mL, and follows the regression equation of $(A_*\text{-}A_0)/A_* = 0.61701C + 0.30403$ (U/mL, $R^2 = 0.992$). Furthermore, the detection limit has also been calculated to be 0.0885 U/mL by the interpolation of the mean plus three times the standard deviation of the zero standards, which is lower than the previous report[36]. The detection precision has been investigated according to the slope of the regression of PTP1B (from 0.1 U/mL to 0.9 U/mL). For each concentration of enzyme, the measurement has been repeated for at least three times independently. The *RSD* of the three slopes is 2.03%, indicating that the precision and reproducibility of the proposed method are acceptable.

3.4 Evaluation for PTP1B inhibitor

It has been reported that BA[37] and Na_3VO_4[38] are separately common non-competitive and competitive inhibitor of PTP1B. In order to test and verify that the proposed method can be applied for the screening of PTP1B inhibitors, the two compounds have been chosen as the model compounds in this study.

As exhibited in Fig. 3(a), with increasing BA concentrations from 0 to 50 μM, the absorbance values decrease gradually. BA can prevent the cleavage of APP/MNPs into AP/MNPs by the enzyme, which will lead to the increasing concentration of TC/AuNPs in the supernatant solution. Meanwhile, it is found that PTP1B activity can be inhibited by 45 μM BA to the utmost extent, since there is no evident change of inhibitory ratio (Fig. 3(b)). Furthermore, the maximum inhibition ratio of BA is 89.29% with the IC_{50} value of 30 μM.

As illustrated in Fig. 3(c), with the increasing Na_3VO_4 concentrations from 0 μM to 10 μM, the absorbance values decrease gradually. As a common competitive inhibitor, Na_3VO_4 is generally

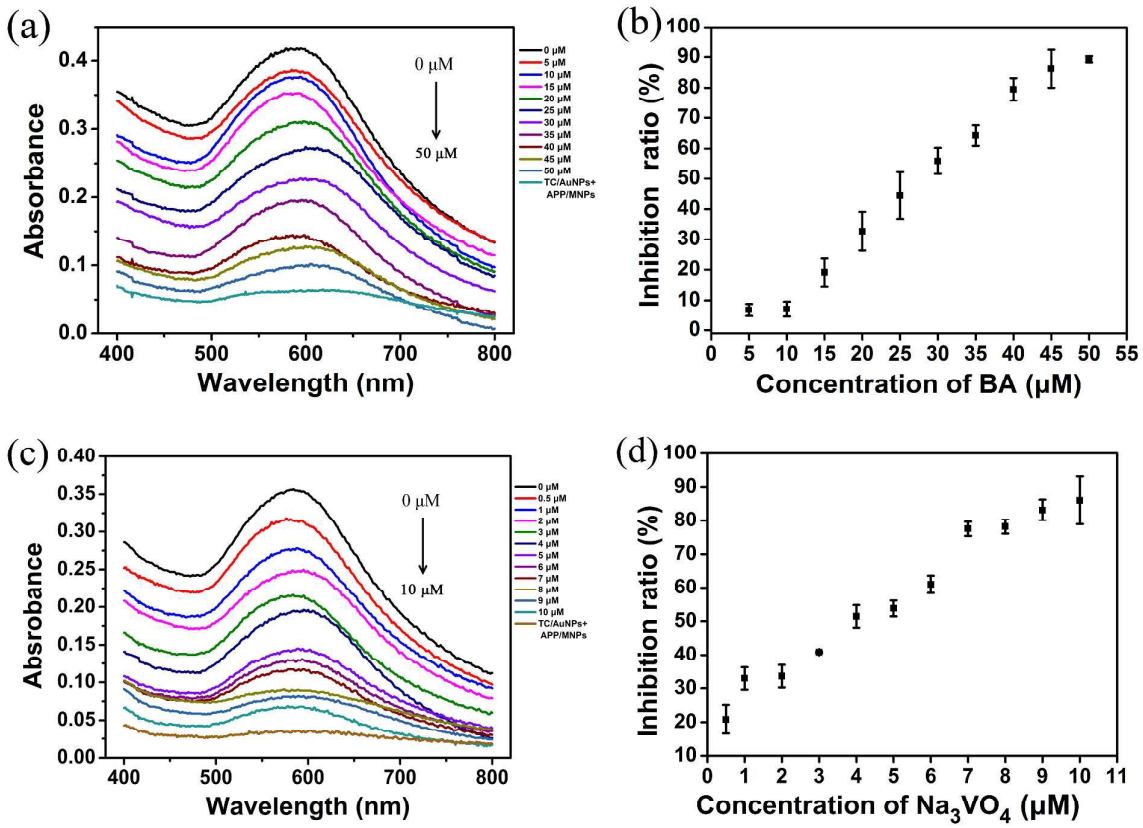

Fig. 3 UV-vis spectra upon analyzing various concentrations of (a) BA and (c) Na_3VO_4. The BA concentrations were 0, 5, 10, 15, 20, 25, 30, 35, 40, 45, and 50 μM. The Na_3VO_4 concentrations were 0, 0.5, 1, 1, 3, 4, 5, 6, 7, 8, 9 and 10 μM. Inhibition ratio versus the concentration of inhibitors: (b) BA and (d) Na_3VO_4.

thought to bind as a transition state analog to the phosphoryl transfer enzymes[32], so as to hinder the cleavage of phosphate ester. Meanwhile, it should be noticed that upon adding 7 μM Na_3VO_4, PTP1B activity can be inhibited extremely, owing to no obvious change of inhibitory ratio (Fig. 3(d), from 7 μM to 10 μM). The maximum inhibition ratio of Na_3VO_4 is 86.05%, with an IC_{50} value of 4 μM.

4 Conclusions

The adsorption between TC and phosphate groups has been exploited for PTP1B activity assay and the inhibitor screening. The method owns the advantages in terms of its low technical and instrumental demands, simple and rapid operation. Moreover, this method can be used as a versatile method for the detection of kinase and phosphatases activity and the corresponding inhibitor screening.

Acknowledgements

This work is supported by the National Natural Science Foundation of China (Grant Nos. 31101354 and 21235003) and the Innovation Program of Shanghai Municipal Education Commission (No. 15ZZ048).

References

1 R. Villaseñor, H. Nonaka, P. D. Zerial, Y. Kalaidzidis and M. Zerial, *eLife*, 2015, **4**, e06156.
2 Y. Zhou, M. Trebak and D. L. Gill, *Mol. Cells*, 2015, **58**, 197-199.
3 C. H. Lu, K. Liu, L. P. Tan and S. Q. Yao, *Chem. Euro. J.*, 2012, **18**, 28-39.
4 I. S. Shin, R. Chand, S. W. Lee, H. W. Rhee, Y. S. Kim and J. I. Hong, *Anal. Chem.*, 2014, **86**, 10992-10995.
5 L. Andersson, *J. Chromatogr. A*, 1991, **539**, 327-334.
6 T. S. Nuhse, *Mol. Cell. Proteomics*, 2003, **2**, 1234-1243.
7 X. S. Li, J. H. Wu, Y. Zhao, W. P. Zhang, Q. Gao, L. Guo, B. F. Yuan and Y. Q. Feng, *J. Chromatogr. A*, 2011, **1218**, 3845-3853.
8 W. Ma, Y. Zhang, L. Li, Y. Zhang, M. Yu, J. Guo, H. Lu and C. Wang, *Adv. Funct. Mater.*, 2013, **23**, 107-115.
9 S. Cazalbou, G. Bertrand and C. Drouet, *J. Phys. Chem. B*, 2015, **119**, 3014-3024.
10 Y. J. Wang, R. J. Sun, A. Y. Xiao, S. Q. Wang and D. M. Zhou, *Geoderma*, 2010, **156**, 237-242.
11 L. Shen, J. Chen, N. Li, P. He and Z. Li, *Anal. Chim. Acta*, 2014, **839**, 83-90.
12 T. Lou, Z. Chen, Y. Wang and L. Chen, *ACS Appl. Mater. Inter.*, 2011, **3**, 1568-1573.
13 G. H. Chen, W. Y. Chen, Y. C. Yen, C. W. Wang, H. T. Chang and C. F. Chen, *Anal. Chem.*, 2014, **86**, 6843-6849.
14 S. Ge, F. Liu, W. Liu, M. Yan, X. Song and J. Yu, *Chem.*

Commun., 2014, **50**, 475-477.
15 Z. Wang, R. Lévy, D. G. Fernig and M. Brust, *J. Am. Chem. Soc.*, 2006, **128**, 2214-2215.
16 C. Chen, C. Zhao, X. Yang, J. Ren and X. Qu, *Adv. Mater.*, 2010, **22**, 389-393.
17 J. J. Storhoff, A. D. Lucas, V. Garimella, Y. P. Bao and U. R. Müller, *Nat. Biotechnol.*, 2004, **22**, 883-887.
18 J. Nam, N. Won, H. Jin, H. Chung and S. Kim, *J. Am. Chem. Soc.*, 2009, **131**, 13639-13645.
19 X. Y. Liu, F. Cheng, Y. Liu, W. G. Li, Y. Chen, H. Pan and H. J. Liu, *J. Mate. Chem.*, 2010, **20**, 278-284.
20 S. I. Yusa, K. Fukuda, T. Yamamoto, Y. Iwasaki, A. Watanabe, K. Akiyoshi and Y. Morishima, *Langmuir*, 2007, **23**, 12842-12848.
21 C. Jeffrey, *Chem. Commun.*, 2007, **36**, 3729-3731.
22 L. M. Rossi, N. J. Costa, F. P. Silva and R. Wojcieszak, *Green Chem.*, 2014, **16**, 2906-2933.
23 A. Salmeen, J. N. Andersen, M. P. Myers, N. K. Tonks and D. Barford, *Mol. cell*, 2000, **6**, 1401-1412.
24 H. Ding, Y. Zhang, C. Xu, D. Hou, J. Li, Y. Zhang, W. Peng, K. Zen, C. Y. Zhang and X. Jiang, *Diabetologia*, 2014, **57**, 2145-2154.
25 H. Lee, J. S. Yi, A. Lawan, K. Min and A. M. Bennett, *Semin. Cell Dev. Biol.*, 2015, **37**, 66-72.
26 A. Haque, J. N. Andersen, A. Salmeen, D. Barford and N. K. Tonks, *Cell*, 2011, **147**, 185-198.
27 A. A. Lanahan, D. Lech, A. Dubrac, J. Zhang, Z. W. Zhuang, A. Eichmann and M. Simons, *Circulation*, 2014, **130**, 902-909.
28 H. Park, B. R. Bhattarai, S. W. Ham, H. Cho, *Eur. J. Med. Chem.*, 2009, **44**, 3280-3284.
29 Q. Xiao, R. Luechapanichkul, Y. Zhai and D. Pei, *J. Am. Chem. Soc.*, 2013, **135**, 9760-9767
30 J. V. Ameijde, J. Overvoorde, S. Knapp, J. D. Hertog, R. Ruijtenbeek and R. M. Liskamp, *Anal. Biochem.*, 2014, **448**, 9-13.
31 C. Liu, F. Wang, Y. Wang, Z. Li, *Chem. Commun*. 2014, **50**, 13983-13986.
32 F. Wang, C. Liu, Y. Fan, Y. Wang, Z. Li, *Chem. Commun*. 2014, **50**, 8161-8163.
33 X. Zhu, C. Feng, Z. Ye, Y. Chen and G. Li, *Sci. Rep.*, 2014, **4**, 4169.
34 E. Cheraghipour, A. M. Tamaddon, S. Javadpour and I. J. Bruce, *J. Magn. Magn. Mater.*, 2013, **328**, 91-95.
35 Y. T. Zhu, X. Y. Ren, Y. M. Liu, Y. Wei, L. S. Qing and X. Liao, *Mater. Sci. Eng. C, Mater. Biol. Appl.*, 2014, **38**, 278-285.
36 L. Fang, J. Cao, L. Duan, Y, Tang, Y. Zhao, *J. Funct. Foods*, 2014, **9**, 264-270.
37 D. Li, W. Li, K. Higai and K. Koike, *J. Nat. Med.*, 2014, **68**, 427-431.
38 G. Huyer, S. Liu, J. Kelly, J. Moffat, P. Payette, B. Kennedy, G. Tsaprailis, M. J. Gresser and C. Ramachandran, *J. Biol. Chem.*, 1997, **272**, 843-851.